Thermodynamic, transport and magnetic properties of α'-NaV_2O_5

J. Hemberger, M. Lohmann, M. Nicklas, A. Loidl
M. Klemm, G. Obermeier and S. Horn

Institut für Physik, Universität Augsburg - D-86135 Augsburg, Germany

Abstract. – We report on heat capacity, electrical resistance and high-temperature ESR experiments on the spin-Peierls compound α'-NaV_2O_5. The spin susceptibility at high temperatures ($T > 250$ K) closely follows a Bonner-Fisher behavior with an exchange interaction $J = 578$ K, but differs significantly from this predictions at lower temperatures. The temperature dependence of the heat capacity can be explained assuming a sum of a linear (magnetic) and a Debye (lattice) contribution. The specific-heat jump at $T_{SP} \approx 35$ K cannot be described by the opening of a gap in mean-field approximation. The release of entropy is almost by a factor of 20 too high compared to the MF predictions of the Bonner-Fisher model for a uniform AFM spin chain with an exchange interaction of $J = 578$ K. The electrical resistance $R(T)$ can roughly be described by variable-range hopping processes and a large anomaly at the transition into the low-temperature dimerized state. From these observations we conclude that the phase transition in α'-NaV_2O_5 at 35 K cannot be explained by a spin-Peierls transition alone.

α'-NaV_2O_5 has been characterized as an inorganic $S = \frac{1}{2}$ one-dimensional antiferromagnet ($\frac{1}{2}$-1DAFM) which reveals a spin-Peierls (SP) transition at low temperatures [1]-[3]. At $T_{SP} = 33.5$ K a transition into a non-magnetic singlet ground state occurs via a dimerization of the spin chains induced by spin-phonon coupling [3]. α'-NaV_2O_5 crystallizes in an orthorhombic structure (space group $P2_1mn$ [4]) and since now it was generally accepted that in this structure magnetic $V^{4+}O_5$ ($S = \frac{1}{2}$) chains along the crystallographic b-axis are separated by non-magnetic $V^{5+}O_5$ chains. However, recent single-crystal diffraction and Raman data raised some doubts if this description in terms of charge ordered chains is correct [5]. Susceptibility data were reported by Isobe and Ueda [1] and Mila *et al.* [6] on polycrystalline samples and by Weiden *et al.* [3] on single crystals. From the high-temperature susceptibility the next-nearest–neighbour exchange coupling was estimated to be 560 K [1] or 529 K [6]. While the susceptibility data of ref. [6] reveal large contributions from paramagnetic defect states, which prevent an analysis of the exponential decay below T_{SP}, the dc susceptibility from Isobe and Ueda [1] exhibits the characteristic features of a one-dimensional spin chain undergoing a spin-Peierls transition. The high-temperature susceptibility data (100 K $< T <$ 700 K) could be well described with a 1D AFM Heisenberg model [1]. In the dimerized state a

gap value between the singlet ground state and the triplet excited state of 85 K has been determined [3]. Further evidence on the SP transition has been provided utilizing X-ray and neutron techniques [2], Raman techniques [3] and NMR experiments [7]. From the neutron experiments an ordering wave vector $q = (0.5, 0.5, 0.25)$ and a gap energy of 114 K [2] were estimated. From the temperature dependence of the spin susceptibility below the SP transition temperature the singlet-triplet gap $\Delta = 98$ K has been determined [7].

An early ESR study of NaV_2O_5 has been reported by Ogawa *et al.* [8]. They observed no anomalous behaviour in the temperature dependence of the ESR spin susceptibility and interpreted their results in terms of a spin-singlet state due to the formation of bipolarons [8]. Recently a number of ESR investigations of α'-NaV_2O_5 have been reported [9]-[11]. The experiments using V^{4+} as ESR probe were conducted at 9.2 GHz [9], 36.2 GHz [10] and 134 GHz [11]. Consistently, the experiments could be described assuming that the V^{4+} ($S = \frac{1}{2}$) ion is exposed to strong ligand fields yielding a configuration $(d_\varepsilon\ )^1$, with slightly anisotropic g-values just below the free-electron value $g = 2$. Gap values Δ of 100 K [9], 92 K [10] and 85 K [12] have been reported. In the dimerized phase the low-frequency spin susceptibilities could be well described with the model from Bulaevskii [12] using alternating exchange constants $J1/J2 \approx 0.8$ [9], [10].

In this article we report on specific heat, electrical resistivity and high-temperature ESR experiments on α'-NaV_2O_5. From these experiments the entropy of the spin-Peierls transition, a characterization of the electronic transport properties and deviations from the linear chain behaviour in the magnetic susceptibility are deduced.

The ESR and resistivity experiments were performed on a high-quality needle-shaped single crystal with a volume of approximately $3 \times 0.1 \times 0.5$ mm^3. The heat capacity experiments were performed using approximately 200 mg of polycrystalline material. The single-crystal preparation has been reported earlier [9]. The heat capacity experiment was performed in a home-built adiabatic Nernst calorimeter operating between 2 K and 100 K. The ESR measurements were made with a Bruker ELEXSYS E500 CW spectrometer at X-band frequency (9.2 GHz). Here a He-flow cryostat allowed measurements between 4 K and room temperature and a nitrogen-flow heating system operates up to 650 K. The electrical resistance was measured with high-impedance electrometers. For temperatures $T > 100$ K a four-probe geometry and excitation voltages well below 10 V were used. In the low-temperature measurements ($20\ \text{K} < T < 80\ \text{K}$) an excitation voltage of 500 V was used in two-probe geometry.

To determine the strength of the exchange interaction we performed ESR experiments up to 650 K. The ESR intensity is a direct measure of the spin-susceptibility and can be analyzed in terms of the time-honored Bonner-Fisher behaviour [13]. Deviations from the model predictions will provide some first hints on possible deviations from a linear-chain behaviour with next-nearest exchange interactions only. Figure 1 shows the temperature dependence of the spin susceptibility as obtained by the present ESR experiments on a single crystal of α'-NaV_2O_5. For $T > 50$ K the susceptibility reveals the characteristic signature of a one-dimensional spin chain with a maximum close to 350 K. The absolute susceptibility scale was determined by comparing the room temperature value of the ESR data to SQUID measurements on the same single crystal. The overall behaviour of the susceptibility is in good agreement with dc results [1]. But closer inspection reveals significant discrepancies. We tried to fit the ESR results with the Bonner-Fisher (BF) model. The result is shown as a solid line in fig. 1. For $T > 250$ K the temperature dependence of the spin susceptibility can be well described assuming a single exchange constant $J = 578$ K. But also the maximum value of the susceptibility $\chi_{\max}$ is in good agreement with BF predictions. According to the model predictions $\chi_{\max} \approx 0.147 g^2 \mu_B^2 / J \approx 4 \times 10^{-4}$ emu/mole is expected close to the experimentally observed value $\chi_{\max} \approx 4.2 \times 10^{-4}$ emu/mole.

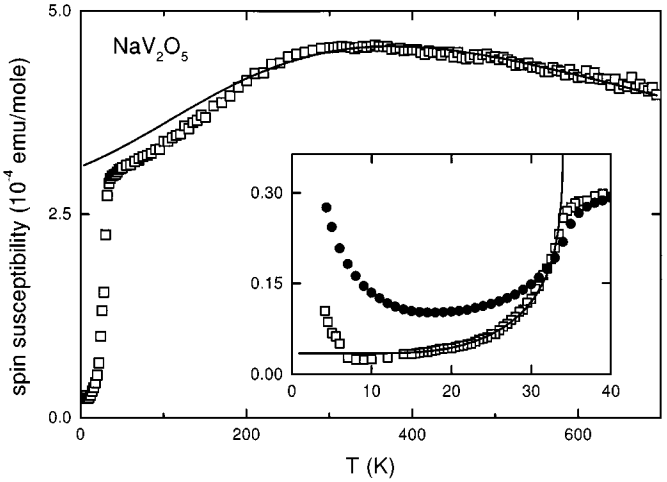

Fig. 1. – Temperature dependence of the ESR spin intensity in single-crystalline α'-NaV_2O_5 (open squares) as compared to the predictions of the Bonner-Fisher model (solid line). The susceptibilities were scaled arbitrarily to 1 at $T = 300$ K. Inset: Temperature dependence of the spin susceptibility at low temperatures around the spin-Peierls transition T_{SP}. The open squares represent the single-crystal data. The solid line is a MF calculation with a gap of 100 K. The full symbols represent the spin susceptibility of the polycrystal that has been used for the specific-heat experiment.

While we find a good agreement with the high-temperature spin susceptibility, the experimental data decrease significantly faster towards lower temperatures. One possible explanation could be the increasing importance of three-dimensional exchange interactions. But the discrepancy could also be due to an alternating or frustrated exchange interaction along the spin chain. In the inset of fig. 1 we present the low-temperature data. For the single crystal that has been used in the ESR and electrical-transport investigations, the ESR results (open symbols) closely resemble those published earlier [9]. The temperature dependence of the spin susceptibility can be described well assuming a spin-Peierls transition temperature of 34 K and an exponential decrease with a gap value of 100 K (solid line in the inset of fig. 1 [9]). The slight increase of the spin susceptibility below 7 K signals a small amount of paramagnetic defect states. For comparison and for a characterization of the polycrystalline material that has been used in the heat capacity experiments, the inset of fig. 1 also shows the temperature dependence of the spin susceptibility for the polycrystal (full symbols). The onset of the spin-Peierls transition seems to be shifted slightly towards higher temperatures ($T_{SP} \approx 35$ K) and is smeared out indicating a distribution of Na stochiometries about the ideal value of one. Clearly, much more defect states are present in the polycrystalline material, a fact that should be taken into account when interpreting the specific-heat results.

The heat capacity of a 1D $S = \frac{1}{2}$ AFM can be described using a sum of magnetic and lattice contributions. The magnetic contribution from the uniform AFM spin chain is given by $C_m = \gamma T \approx 0.7R \times k_B T/J$ [13], where J is the exchange integral ($J = 578$ K) and R the molar gas constant. The lattice contribution can be calculated using the Debye integral in which the specific heat at all temperatures can be calculated in terms of the Debye temperature Θ_D. This model yields a Debye-like T^3-dependence at the lowest temperatures ($T \ll \Theta$), as expected from the phonon contributions in a crystalline material and levels off to a constant value corresponding to the number of degrees of freedom at high temperatures ($T \geq \Theta$). Below a SP transition a gap opens in the spin excitation spectrum and the linear magnetic contribution

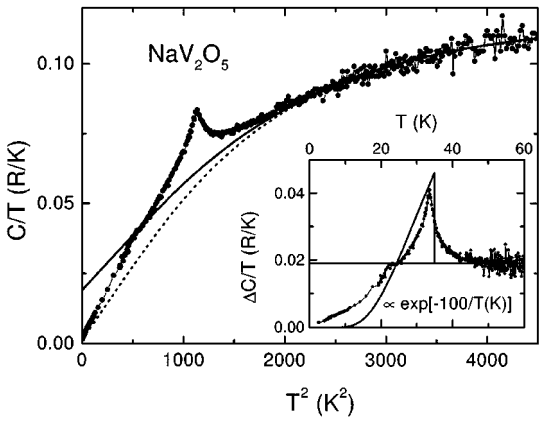

Fig. 2. – Heat capacity in α'-NaV_2O_5 plotted as C/T *vs.* T^2. The solid line (scenario B) was calculated to produce a mean-field–like jump in the specific heat compatible with the experimental results. The dashed line (scenario A) has been calculated with a linear magnetic contribution as predicted by the Bonner-Fisher model. Inset: Heat capacity plotted as C/T *vs.* T, with the lattice contribution of scenario A subtracted. The solid line reveals the value of the linear term. The dashed line represents a MF-like jump of the heat capacity at a phase transition temperature $T_{\rm SP} = 35$ K and an exponential decay, assuming a gap value of 100 K.

is expected to decrease exponentially towards the lowest temperatures. In the mean-field (MF) approximation the jump in the heat capacity should be $\Delta C = 1.43\gamma T_{\rm SP}$. From earlier investigations it was already clear that strong deviations from this behaviour have to be expected. While the MF result predicts a ratio $2\Delta/k_{\rm B}T_{\rm SP} = 3.52$, a value of 5.9 has been detected experimentally [9].

The heat capacity of α'-NaV_2O_5 for temperatures 3 K $< T <$ 70 K is shown in fig. 2. We used the representation C/T *vs.* T^2 to provide some experimental evidence of the existence of a linear and a cubic term. However, fig. 2 clearly shows the problems for any consistent analysis of the magnetic linear-in-T specific-heat term which should be present for $T > T_{\rm SP}$. Due to the high spin-Peierls transition temperature the phonon contribution is high and shows significant deviations from a T^3-dependence. In addition, the linear behaviour of the magnetic specific heat strictly holds only for temperatures up to the order $J/10k_{\rm B}$ ($\approx$ 50 K) [13]. In the analysis of our specific-heat results we tried two parameterizations to describe the data for $T > T_{\rm SP}$: In scenario A we fixed the linear term to the value which can be calculated from the exchange interaction, namely $\gamma = 1.21 \times 10^{-3} R/K$ and fitted the phonon contribution with two parameters, *i.e.* the Debye temperature and the degrees of freedom N. The result is shown as dashed line in fig. 2. The best fit was obtained using a Debye temperature $\Theta_{\rm D} = 281$ K and $N = 15$. In this case the specific-heat anomaly at $T_{\rm SP}$, $\Delta C/\gamma T_{\rm SP} \approx 20$, far off the MF value.

In scenario B we tried to check if the data are at least compatible with a MF description of a spin-Peierls transition. The solid line in fig. 2 shows the model predictions for C/T *vs.* T^2 were we fixed the magnetic specific heat to the mean-field prediction $\Delta C/\gamma T_{\rm SP} \approx 1.4$, to reproduce the MF jump in the specific heat. From the fit in scenario B we deduced $\gamma = 0.019R/K$, $\Theta_{\rm D} = 302$ K and $N = 14$. The temperature dependence of the magnetic contribution dc is shown in the inset of fig. 2. The solid line represents the linear contribution of the spin chain. In addition, we calculated the exponential decrease of the specific heat with a temperature independent gap value of 100 K. Here we assumed that $T_{\rm SP} = 35$ K, in good agreement with the ESR results for the polycrystalline material (see inset of fig. 1). The shape of the

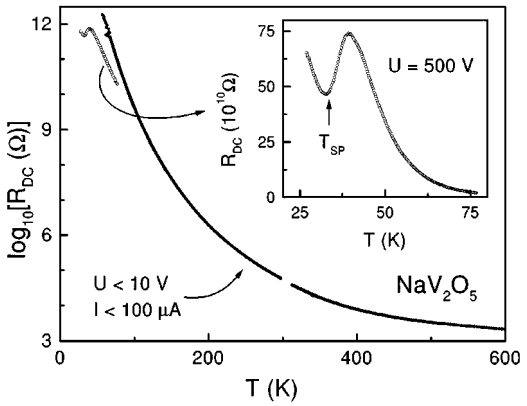

Fig. 3

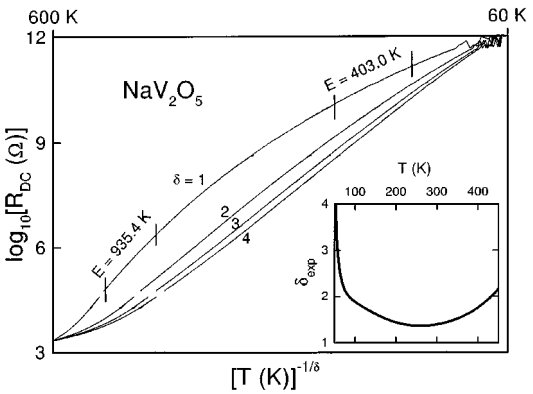

Fig. 4

Fig. 3. – Temperature dependence of the electrical resistance in α'-NaV_2O_5. The inset shows the low-temperature resistivity as determined at high excitation voltages in two-probe geometry.

Fig. 4. – Logarithm of the resistance *vs.* $T^{-1/\delta}$ with $\delta = 1, 2, 3$ and 4. Note that for each value of the exponent only the end points of the scale coincide. The inset shows the temperature dependence of the exponent parameter δ. The given energy barriers for thermally activated behaviour are evaluated from the marked areas of the $\delta = 1$ curve.

specific-heat anomaly reveals the signature of a first-order phase transition. In addition, for temperatures below 20 K there is a strong excess specific heat. However, as it became clear from the spin susceptibility, the sample which has been used for the specific-heat investigations contains a considerable amount of free spins, and hence this excess heat capacity should not be overestimated. This model calculations according to scenario B seem to be roughly compatible with the experimental results. But now the linear term is a factor of 15 too large compared to the predictions of the Bonner-Fisher model for a uniform AFM spin chain. Therefore, it has to be clearly stated that the release of entropy at the phase transition is far too high for a spin-Peierls system with an exchange constant $J = 578$ K and there exist significant and severe discrepancies between experiment and MF model predictions. For $CuGeO_3$, the other inorganic spin-Peierls compound, the heat capacity roughly can be described using a MF approach [14].

The resistivity along the chain direction is plotted in fig. 3. The resistivity reveals a clear semiconducting behaviour and increases from $10^3\Omega$ at 600 K to almost $10^{13}\Omega$ at low temperatures. Due to a large number of microcracks in the single crystalline sample we did not attempt to calculate the specific resistance. With relatively low excitation voltages and in four-probe geometry we were able to follow the resistance down to 50 K. In order to see if the spin-Peierls transition can be detected in the electrical resistivity, we measured with high excitation voltages down to 20 K (inset in fig. 3). A clear but smeared out anomaly can be detected. The minimum of $R(T)$ corresponds to the phase transition temperature. The strong decrease of the resistance by almost 40% in a temperature range of 5 K above the spin-Peierls transition could be explained by a fluctuation-driven delocalization of charge carriers just above the phase transition temperature or by structural effects. However, $R(T)$ increases again below T_{SP} for decreasing temperature, again indicating semiconducting behaviour.

For a closer inspection of the nature and the dimensionality of the charge transport in α'-NaV_2O_5, fig. 4 shows $\log(R)$ *vs.* $T^{-1/\delta}$ ($\delta = 1, 2, 3$ and 4). Here $\delta = 1$ corresponds to purely

thermally activated transport while the exponents $\delta = 2, 3$ and 4 describe variable-range hopping (VRH) in 1, 2 and 3 dimensions, respectively. Figure 4 shows that either of these dependences, which would correspond to straight lines in the representation of fig. 4, describe the experimental results in narrow temperature ranges only. This fact becomes even more clear, when the exponent is followed as a function of temperature (inset of fig. 4). For high temperatures δ is of the order of 2, indicative for one-dimensional transport, but it increases strongly towards T_{SP}.

In conclusion, we have presented heat capacity, electrical transport and spin susceptibility data in NaV_2O_5. The resistivity data reveal semiconducting behaviour and the transport at high temperatures can roughly be described by a one-dimensional hopping process. Below 100 K, 3D hopping seems to become important. Even when taking into account the problems of an analysis which are mainly due to the high transition temperature, we show that the calorimetric data are not compatible with a specific-heat jump as predicted in MF theory for a SP transition. The resulting linear term is much too large for a 1D AFM chain. At present we cannot give a satisfactory description of the experimentally observed heat capacity in terms of a pure spin-Peierls transition. The spin susceptibility at high temperatures can be well described using the Bonner-Fisher model for a uniform AFM $S = \frac{1}{2}$ spin chain. Significant deviations appear below 250 K.

We acknowledge stimulating discussions with B. Elschner, B. Lüthi, A. P. Kampf, W. Trinkl and M. Dumm. This work has been partly supported by the BMBF under the contract number EKM/13 N 6917.

REFERENCES

[1] Isobe M. and Ueda Y., *J. Phys. Soc. Jpn.*, **65** (1996) 1178.

[2] Fujii Y., Nakao H., Yosihama T., Nishi M., Nakajima K., Kakurai K., Isobe M., Ueda Y. and Sawa H., *J. Phys. Soc. Jpn.*, **66** (1997) 326.

[3] Weiden M., Hauptmann R., Geibel C., Steglich F., Fischer M., Lemmens P. and Güntherodt G., *Z. Phys. B*, **103** (1997) 1.

[4] Carpy A. and Galy J., *Acta Crystallogr. Sect. B*, **31** (1975) 1481.

[5] Smolinski H., Gros C. Weber W., Peuchert U., Roth G., Weiden M. and Geibel C., preprint cond-mat/9801276.

[6] Mila F., Millet P. and Bonvoisin, J., preprint cond-mat/9605024, v2.

[7] Ohama T., Isobe M., Yasuoka H. and Ueda Y., *J. Phys. Soc. Jpn.*, **66** (1997) 545.

[8] Ogawa K., Onoda M. and Nagasawa H., *J. Phys. Soc. Jpn.*, **55** (1986) 2129.

[9] Lohmann M., Loidl A., Klemm M., Obermeier G. and Horn S., to be published in *Solid State Commun.*

[10] Vasilev A. N., Smirnov A. I., Isobe M. and Ueda Y., *Phys. Rev. B*, **56** (1997) 5065.

[11] Schmidt S., Palme W. and Lüthi, B., preprint; Palme W., Schmidt S., Lüthi B., Boucher J. P., Weiden M., Hauptmann R., Geibel C., Revcolevschi A. and Dhalenne G., to be published in *Physica B.*

[12] Bulaevskii L. N., *Sov. Phys. Solid State*, **11** (1969) 921.

[13] Bonner J. C. and Fisher M. E., *Phys. Rev. A*, **135** (1962) 640; in our definition the exchange constant corresponds to $2J$.

[14] Lasjaunias J. C., Monceau P., Rémenyi, Sahling S., Dhalenne G. and Revcolevschi M. E., *Solid State Commun.*, **101** (1997) 677.